International Journal of Nanomedicine

Dovepress
Taylor & Francis Group

Open Access Full Text Article

ORIGINAL RESEARCH

Engineered Hybrid Nanovesicles Combining Macrophage Membranes and Artificial Lipids for Abdominal Aortic Aneurysm Therapy

Weiyao Chen[1,*], Jiling Zhao[2,*], Jiamin Xu[2,*], Heng Wu[2,*], Zhongnan Xia[2], Jie Liu[2], Shilong Sun[3], Yuhua Lei[2], Hongbo Chen[4], Jiaqi Yu[5], Jiaxin Hu[2,6]

[1]Department of Nutrition, The First Affiliated Hospital of Sun Yat-Sen University, Guangzhou, Guangdong, People's Republic of China; [2]Cardiovascular Disease Center, The Central Hospital of Enshi Tujia and Miao Autonomous Prefecture, Enshi Clinical College of Wuhan University, Enshi, Hubei, People's Republic of China; [3]Department of Vascular Surgery, The First Affiliated Hospital, Zhejiang University School of Medicine, Hangzhou, Zhejiang, People's Republic of China; [4]Department of Urology, Central Hospital of Enshi Tujia and Miao Autonomous Prefecture, Enshi, Hubei, People's Republic of China; [5]Department of Cardiology, The Second Affiliated Hospital of Wenzhou Medical University, Wenzhou, Zhejiang, People's Republic of China; [6]Hubei Selenium and Human Health Institute, the Central Hospital of Enshi Tujia and Miao Autonomous Prefecture, Enshi, Hubei, People's Republic of China

*These authors contributed equally to this work

Correspondence: Jiaxin Hu, Cardiovascular Disease Center, The Central Hospital of Enshi Tujia and Miao Autonomous Prefecture, Enshi Clinical College of Wuhan University, No. 158 Wuyang Avenue, Enshi, Hubei, People's Republic of China, Email hjxlmy@outlook.com; Jiaqi Yu, Department of Cardiology, The Second Affiliated Hospital of Wenzhou Medical University, No. 109 West Xueyuan Road, Wenzhou, Zhejiang, People's Republic of China, Email yujiaqi_2018@163.com

Background and Aims: Abdominal aortic aneurysm (AAA) is a vascular condition with high mortality for which no pharmacological treatments have been approved. Targeting endothelial dysfunction as a primary disease initiator, the vascular endothelial cell (VEC)- protective compound Senkyunolide I (SEI) demonstrates therapeutic promise through robust antiapoptotic activity. Nevertheless, SEI's clinical translation faces limitations due to systemic toxicity, necessitating development of safer therapeutic alternatives.

Results: This study presents an engineered biomimetic nanoplatform (Lipo-MM nanoparticles) combining macrophage-derived membranes with synthetic lipid bilayers for targeted SEI delivery. The macrophage membrane component facilitates precise targeting of activated VECs, while optimized artificial membrane fluidity enhances nanoparticle stability. This dual-membrane configuration enables sustained SEI release with enhanced biodistribution, achieving superior cytoprotective effects. Notably, we established a novel fusion membrane delivery system (Lipo-MM/SEI) and validated its therapeutic efficacy in angiotensin II-challenged AAA murine models. The nanocarrier significantly attenuated AAA progression, reflected by decreased 40% of AAA incidence, 31.4% of maximum aortic diameter, reduced elastin degradation and prevented fatal rupture events. Furthermore, Lipo-MM/SEI administration substantially reduced hepatorenal toxicity associated with free SEI administration during chronic treatment.

Conclusion: These results demonstrate that hybrid biomimetic systems integrating natural cellular components with engineered materials offer a strategic approach for vascular endothelial repair therapy while minimizing off-target effects. This membrane fusion technology establishes a prototype for developing next-generation targeted vascular therapeutics.

Keywords: macrophage membranes, liposomes, abdominal aortic aneurysm, anti-inflammatory

Introduction

Abdominal aortic aneurysm (AAA) is a common and potentially life-threatening disease characterized by rapid progression and high acute-phase morbidity,[1,2] with no effective pharmacological treatments available to stop its advancement. Recent studies working on nanoparticle-based targeted therapy for AAA that can halt or regress AAA in animal models.[3,4] Among different nano-carriers developed for improved drug delivery, such as liposomes, carbon nanotubes, dendrimers, polymeric micelles, polymeric conjugates, and nanoparticles, only a few have reached clinical applications. Concerns on the biocompatibility of the

Received: 4 September 2025
Accepted: 10 December 2025
Published: 23 December 2025

carrier limits their clinical application. Pathologically, aortic endothelial cell (EC) activation and apoptosis synergistically drive AAA pathogenesis alongside inflammatory cascades.[5,6] Uncontrolled acute/chronic inflammation exacerbates irreversible aortic damage, while existing surgical options remain insufficient to prevent vascular degeneration due to the absence of multi-functional therapies maintaining vascular homeostasis and counteracting inflammatory cytokines.[7]

Macrophages critically participate in cardiovascular pathologies including atherosclerosis, myocardial infarction, hypertension, and AAA.[8–11] Their role in AAA involves direct substrate interactions and bioactive factor secretion,[12] with vascular endothelial cells (VECs) exhibiting upregulated ICAM-1/VCAM-1 expression upon activation during early AAA stages.[13] These adhesion molecules mediate macrophage recruitment to aortic lesions via integrin α4β1 binding,[14] accelerating vascular dissection progression.[15] Furthermore, lesion-associated macrophages amplify inflammation through cytokine secretion,[16,17] positioning anti-endothelial inflammation strategies as pivotal therapeutic targets.

Senkyunolide I (SEI), a bioactive phthalide derivative from *Ligusticum chuanxiong* and *Angelica sinensis*, demonstrates potent anti-apoptotic properties with therapeutic potential against AAA.[18] However, clinical translation is constrained by non-specific VEC targeting and systemic toxicity. This necessitates innovative delivery systems combining VEC protection and anti-inflammatory action.

Our study developed hybrid biomimetic liposomes (Lipo-MM) by integrating macrophage membranes with synthetic lipid bilayers for targeted AAA therapy (Figure 1). Through controlled extrusion, these nanovesicles preserve macrophage targeting capacity while maintaining physicochemical stability. Capitalizing on lipid bilayer fluidity enabling membrane fusion, Lipo-MM achieves scalable production with optimized macrophage membrane utilization. Comprehensive characterization confirmed Lipo-MM's structural integrity and targeting specificity in both in vitro assays and AngII-induced AAA murine models. SEI-loaded Lipo-MM (Lipo-MM/SEI) exhibited enhanced drug payload

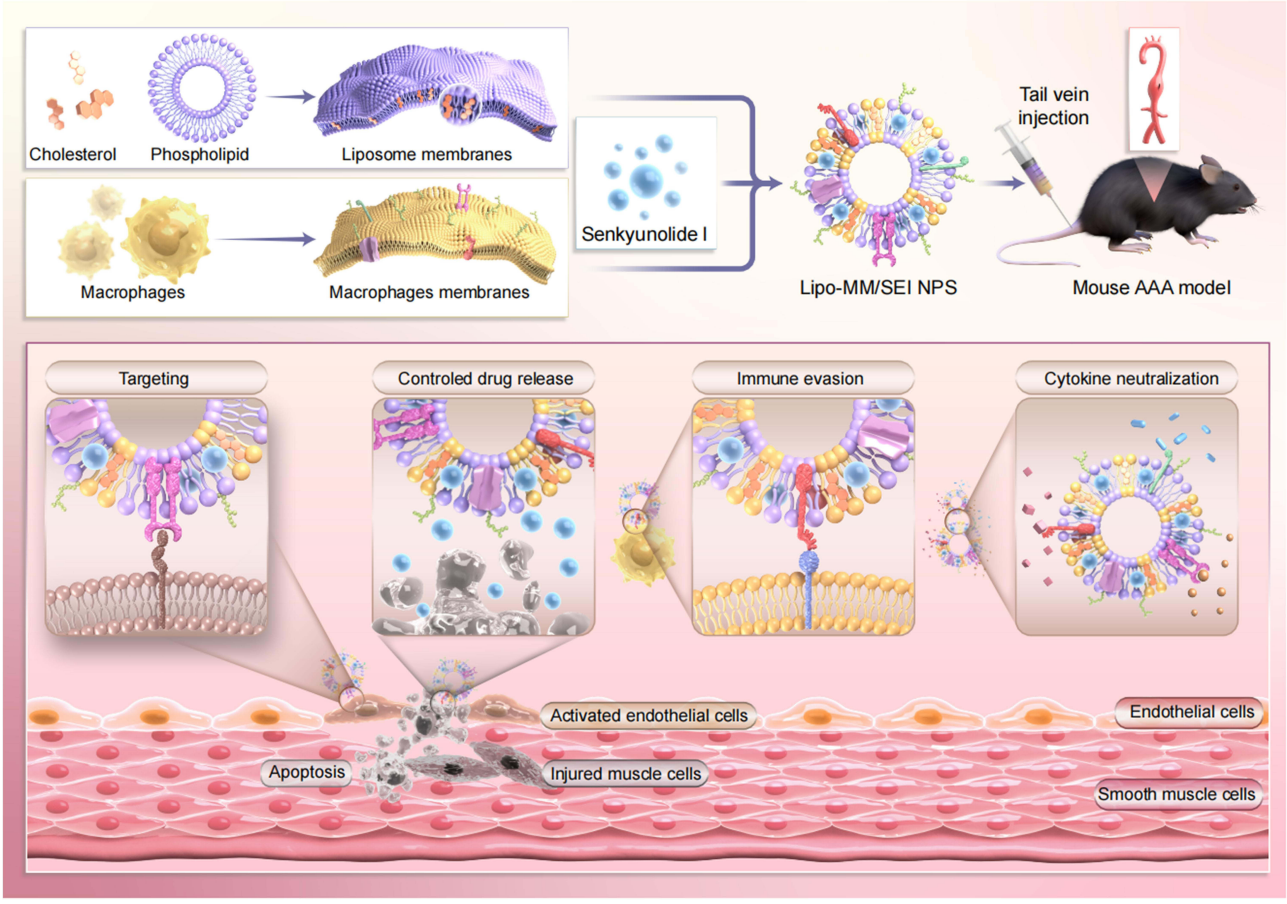

Figure 1 Central illustration. Schematic design and mechanism of Lipo-MM/SEI for targeted AAA therapy.

and therapeutic efficacy in vivo, demonstrating significant potential in preventing AAA progression and rupture. This platform establishes a prototype for precision vascular therapeutics with minimized off-target effects.

Experimental Method

Macrophage Membrane Isolation

RAW264.7 cells and HUVEC (human umbilical vein endothelial cells) were obtained from ATCC and cultured based on manufacturer's instructions. Macrophage membranes were extracted from RAW264.7 cells via a modified hypotonic lysis method.[14] Cells were resuspended in ice-cold hypotonic lysis buffer (10 mM Tris-HCl, 1 mM EDTA, pH 7.4) and underwent four freeze-thaw cycles between liquid nitrogen and 37°C water baths. Cellular debris was eliminated through sequential centrifugation: first, an initial clarification at 850×g for 10 minutes at 4°C, followed by ultracentrifugation of the supernatant at 15,000 × g for 30 minutes at 4°C. The membrane fraction pellet was resuspended in sterile PBS, and protein concentration was measured using a Pierce™ BCA Protein Assay Kit (Thermo Fisher Scientific, USA) with bovine serum albumin as the standard.

Synthesis of Lipo-MM

Synthesis of Lipo-MM involved dissolving DSPE-mPEG2000 and Soya PC in chloroform, followed by forming a film through solvent evaporation using a rotary evaporator. The lipid suspension was passed through cellulose acetate membranes with pore sizes of 100, 200, and 400 nm a total of 10 times, in the presence of MM vesicles to create Lipo-MM or in their absence for the control Lipo. The formulations Lipo-MM/DiD, Lipo-MM/SEI, Lipo/DiD, and Lipo/SEI were all generated by incorporating 2μg of DiD or 500μg of SEI into the soya PC solution, adhering to the same methodology.

Verification of Membrane Fusion

Membrane fusion between macrophages and lipid membranes was evaluated using FRET. DiO and DiI (0.1% w), were integrated into cholesterol and POPC to create liposomes. Raw264.7 cells membranes were merged with DiO- and DiI-labeled liposomes, then subjected to sonication and extrusion. Sample's fluorescence spectrum was recorded at 460nm by Tecan fluorescence spectrometer (Männedorf, Switzerland).

Protein Identification

We quantified the protein content in both the raw macrophage membranes and the final Lipo-MM/SEI nanoparticles using the BCA protein assay, which allowed us to determine the overall efficiency of the membrane-coating process by comparing the total protein amounts and to confirm consistent membrane protein loading across different batches. Protein content in Lipo-MMs was confirmed using SDS-PAGE. The levels of CD14, CD40, TLR4, integrin α4, integrin β1, CD119, CD120a, CD120b, CD126 and CD130 were then analyzed by Immunoblotting analysis.

SEI Release Assay

Sample mixture was enclosed in a 100 kDa MWCO dialysis bag (Sigma-Aldrich, St Louis, MO, USA) containing PBS at pH 7.4 and maintained at 37 °C. At specified intervals, the solution from the bag was extracted, and the SEI concentration was measured with a Tecan spectrophotometer at a 300 nm absorption wavelength.

Inflammatory Cytokine Neutralization

The efficacy of neutralizing inflammatory cytokines IL-6, TNF-α, and IFN-γ was assessed by incubating various concentrations of Lipo-MMs (0, 1, and 3 mg/mL) with TNF-α (370 pg/mL), IL-6 (2000 pg/mL), and IFN-γ (880 pg/mL) in PBS at 37 °C for 30 minutes. Following incubation, samples were centrifuged at 16,000×g for 15 minutes to collect the supernatant. ELISA was used to quantify free inflammatory cytokine levels in the supernatant.

Animal Experimentation

Animal experiments adhered to ARRIVE guidelines and received approval from the Institutional Ethics Committee of the Central Hospital of Enshi Tujia and Miao Autonomous Prefecture (Approval No.202412002). All animal experimental procedures were performed by following the China Animal Welfare Guidelines. Male ApoE$^{-/-}$ mice, aged 8 to 10 weeks, were obtained from Jiangsu Huachuang Xinnuo Medical Technology Co., Ltd. and maintained at the Enshi Central Hospital Animal Experimental Center under controlled conditions of 23°C temperature, 55% humidity, and a 12-hour light/dark cycle. Mice were randomly assigned to one of four groups: AngII + PBS, AngII + free SEI, Lipo/SEI, and Lipo-MM/SEI. Each group received subcutaneous Alzet model 2004 osmotic minipumps for a four-week AngII (Sigma-Aldrich) infusion at 1000 ng kg^{-1} min^{-1}. During the study, animals were maintained on a high-fat diet (20% lard, 10% sucrose, 3% cholesterol, 0.2% bile salts). Upon study completion, mice were anesthetized with 1.5–2% isoflurane and euthanized via cervical dislocation. Blinded investigators excised abdominal aortas for morphological evaluation and conducted analyses including Elastin Van Gieson (EVG) staining, Western blotting, immunohistochemistry, and immunofluorescence.

Biodistribution Imaging

For in vivo tracking, 100 μL of DiD-labeled Lipo or Lipo-MM formulations were administered intravenously for biodistribution imaging. Fluorescence signals were monitored using an IVIS Spectrum imaging system (PerkinElmer) at predefined intervals. Organs were collected 24 hours after injection for ex vivo fluorescence measurement.

Histopathological Analysis

Aortic tissues were preserved in 4% paraformaldehyde for a duration of 24 hours, subsequently embedded in paraffin, and sliced into sections of 4 μm thickness for histopathological examination. To assess inflammation, hematoxylin and eosin (H&E) staining was performed, and two pathologists evaluated the slides independently using a Nikon Eclipse Ci light microscope. For elastin visualization, sections underwent EVG staining with resorcin-fuchsin and methylene blue solutions.

Statistical Analysis

Blinding was performed for all subjective analyses, including histological and imaging analyses. All data were analyzed and graphed using GraphPad Prism 8.0 (GraphPad Software). All values were presented as mean ± SD and plotted as the mean values with SD. Significance levels were set at $*p < 0.05$, $**p < 0.01$, and $***p < 0.001$. Specific tests of statistical significance are detailed in figure legends.

Results and Discussion

Selection, Synthesis, and Characterization of Lipo-MM/SEI Were Conducted

The RAW264.7 murine macrophage membrane was chosen for nanovesicle fabrication because of its proven ability to selectively sequester inflammatory cytokines in activated VECs.[19] Hybrid biomimetic vesicles were fabricated via an optimized thin-film hydration/extrusion protocol adapted from established methodologies.[20] Macrophage membrane isolation was achieved through hypotonic lysis, with the resultant membrane fraction subsequently combined with synthetic lipid components at a 1:5 (w/w) ratio-a formulation empirically validated to preserve post-fusion membrane functionality.[21] This membrane-lipid mixture underwent sequential hydration, sonication, and polycarbonate membrane extrusion to facilitate bilayer fusion. To augment colloidal stability, cholesterol was systematically incorporated into the Lipo-MM architecture during lipid film preparation.

To assess the fusion process, synthetic lipid membranes were tagged with the Förster resonance energy transfer (FRET) dye combination, Dil and DiO, before merging with unlabeled macrophage membranes. The introduction of macrophage membranes resulted in a diminished fluorescence intensity at 565nm (Dil), signifying their fusion with the synthetic lipid membranes and the subsequent decrease in Dil fluorescence (Figure 2A). Raw264.7 cell membranes were labeled with Dil, while lipid membranes were marked with DiD. Figure 2B illustrates that confocal laser scanning microscopy (CLSM) results indicated significant overlap between macrophage membranes and synthetic lipid

membranes. Transmission electron microscopy revealed that the Lipo-MMs were spherical (Figure 2C), akin to traditional Lipos. The Lipo-MMs had a diameter of ~190 nm with a favorable polydispersity index (PDI) of 0.215. The diameter is smaller than that of the extruded MM vesicles (Figure 2D), possibly due to the decreased mechanical rigidity of the macrophage membrane following fusion with the more flexible artificial lipid membrane. Furthermore, the zeta potential of Lipo-MMs was observed to be between that of MM vesicles and Lipos (Figure 2E), indicating successful

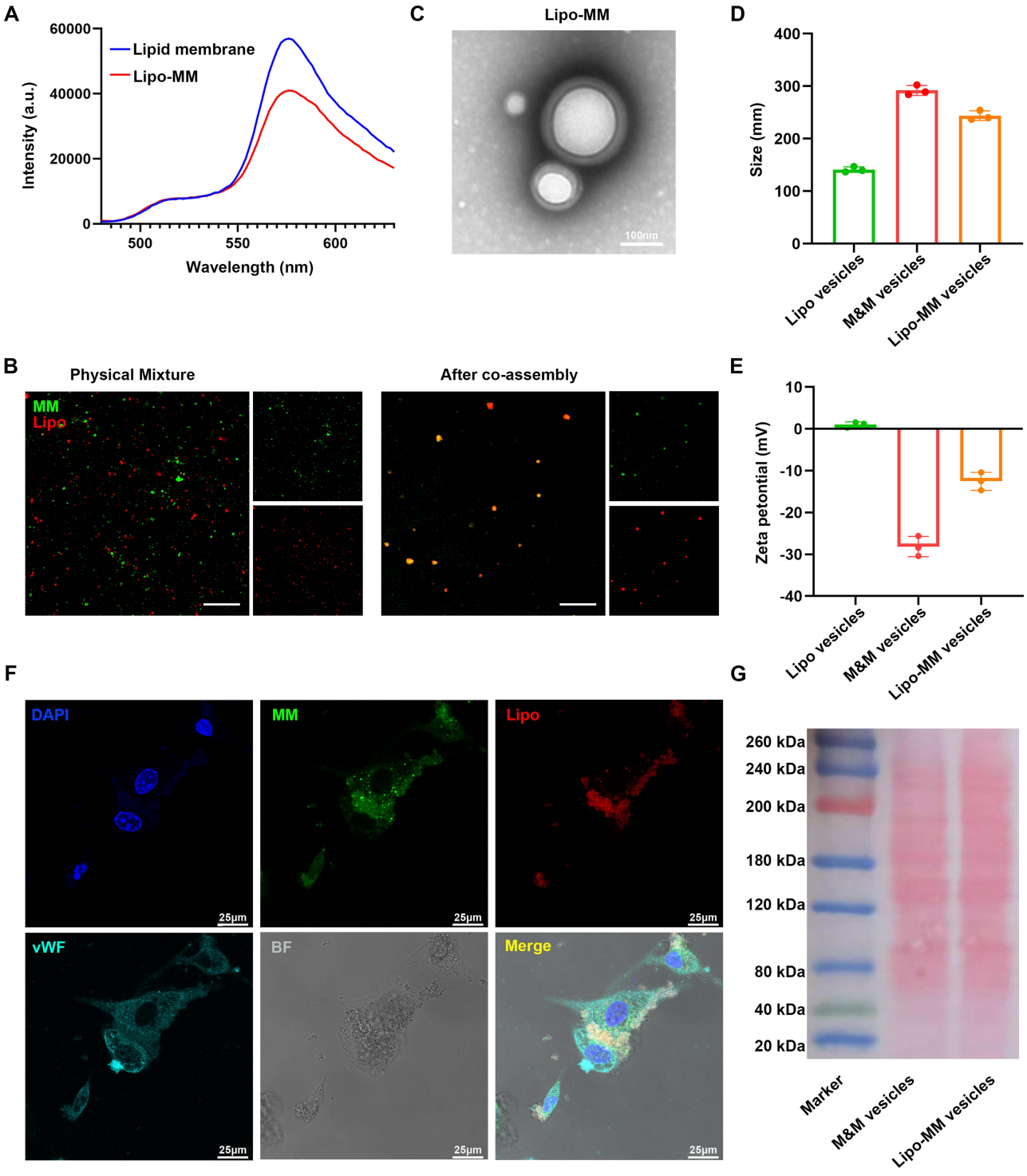

Figure 2 Continued.

https://doi.org/10.2147/IJN.S565290

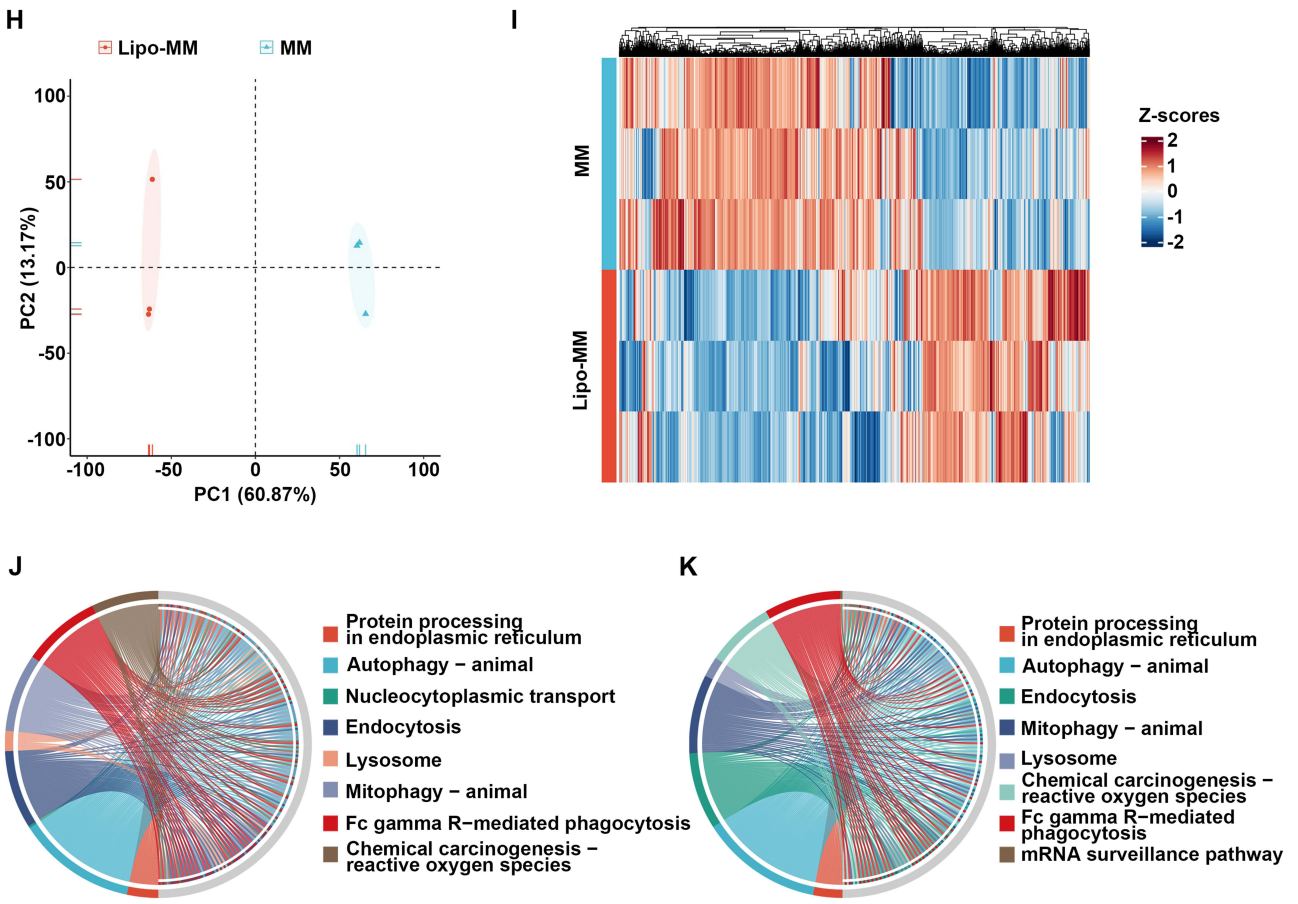

Figure 2 Selection, Synthesis and Characterization of Lipo-MM/SEI. (**A**) The synthetic lipid membranes and the fused macrophage membranes were labeled with FRET dye for DiO and Dil. (**B**) Particle size distribution of Lipo, MM and Lipo-MMs vesicles were assessed by dynamic light scattering (DLS)(mean ± SD, n=3). (**C**) Zeta potential distribution of Lipo, MM and Lipo-MMs vesicles were assessed by DLS (mean ± SD, n=3). (**D**) Confocal laser scanning microscopy (CLSM) image of Lipo-MMs vesicles. (**E**) Transmission electron microscopy (TEM) image of Lipo-MMs vesicles. (**F**) Fluorescence microscopy image of Lipo-MMs vesicles. (**G**) Protein composition of Lipo-MMs vesicles was shown by SDS-PAGE analysis. (**H**) Principal component analysis (PCA) of the proteomic of MM vesicles versus Lipo-MMs vesicles (n=3). (**I**) Clustering heatmap of the differential expressed proteins (DEPs), red indicates high expression protein, blue indicates low expression protein, and each row indicates the expression of each protein in different groups. (**J** and **K**) Circle plot of biological process and cellular components of GO enrichment.

fusion of the macrophage and lipid membranes. In contrast, minimal overlap was observed when the two types of membranes were mixed without fusion. Fluorescently labeled Lipo-MMs were incubated with HUVECs to verify the stability of the drug nanocarrier system. Fluorescence microscopy images showed a strong overlap between the red fluorescence of DiD (representing SEI) and the green fluorescence of DiO (representing Lipo-MMs) (Figure 2F). This colocalization suggests that Lipo-MM/DiD maintained good stability even after being internalized by HUVECs. The drug loading efficiency (LE) and encapsulation efficiency (EE) of Lipo-MM/SEI were 2.78% and 81.2%, respectively. To further explore whether Lipo-MMs can inherit essential physiological characteristics of the originating macrophages, membrane proteins targeting adhesion proteins on activated VECs, including integrin α4 and integrin β1, were analyzed by Western blotting. Additionally, CD47, a protein involved in immune evasion, was detected. As anticipated, following membrane derivation and fusion, Lipo-MMs maintained these proteins, similar to MM vesicles (Figure 2G). These findings demonstrate that the macrophage membranes effectively merged with the synthetic lipid membranes, maintaining the key physiological characteristics of the original macrophages.

A novel method employed 3D-data independent acquisition to analyze the protein composition of MMs and Lipo-MMs vesicles. PCA was utilized to reduce data dimensionality by transforming data into principal components, preserving most of the variance. PCA indicated significant differences between Lipo-MM hybrid vesicles and MM vesicle groups (Figure 2H). A query of the UniProt database identified 6,399 membrane proteins in the Lipo-MM hybrid

vesicles (Figure 2H). Clustering heatmap for differentially expressed proteins in Lipo-MMs vesicles versus MM vesicles (Figure 2I). These proteins were functionally classified according to biological processes and cellular components (Figure 2J and K). We effectively combined macrophage membranes with synthetic lipid membranes, maintaining essential functional proteins from the macrophage membranes. Notably, the flexibility of the synthetic lipid membranes can be adjusted to control the release of encapsulated drugs from Lipo-MMs.

Strategies for Targeting and Evading the Immune System by Lipo-MMs

The in vitro targeting capability of Lipo-MM/DiD towards activated ECs was assessed to determine if biomimetic nanoparticles retained the functional characteristics of macrophage membranes. CLSM images demonstrated that, following a 4-hour co-incubation with activated ECs, Lipo-MM/DiD exhibited greater adhesion to the ECs compared to Lipo/DiD (Figure 3A and B).

The in vitro cellular uptake of Lipo-MM/DiD by macrophages was subsequently assessed. The internalization of Lipo-MM/DiD in RAW 264.7 cells was observed using CLSM following a 4-hour incubation. As depicted in Figure 3C and D, fewer macrophages treated with Lipo-MM/DiD were observed than those treated with Lipo/DiD, indicating reduced uptake. The study indicates that macrophage membrane-derived CD47 proteins effectively prevent macrophages from phagocytosing Lipo-MM/DiD.

The evaluation of targeting Lipo-MM nanoparticles to activated endothelial cells (ECs) was conducted using a mouse model of abdominal aortic aneurysm (AAA). Mice with AAA were administered intravenous injections of equal doses of Lipo/DiD and Lipo-MM/DiD. Twenty-four hours later, aortas were collected for additional fluorescence imaging. The group receiving Lipo-MM/DiD demonstrated notably enhanced DiD dye fluorescence in the aorta in contrast to the faint signals seen in the Lipo/DiD group (Figure 3E). Twenty-four hours post-injection, DiD fluorescence signals were detected in major organs notably the kidneys and liver, likely due to clearance by the mononuclear phagocyte system. The fluorescence signal from the DiD marker was found to be concentrated in the aorta across both experimental groups. However, a significant difference was observed in the liver, where the Lipo/DiD group demonstrated a markedly stronger fluorescence signal. In contrast, the Lipo-MM/DiD group exhibited a significantly diminished signal in the liver, indicating a notable variation in the distribution of the fluorescence between these two groups (as illustrated in Figure 3F). These data indicated that Lipo-MM nanoparticles effectively target the aorta while minimizing accumulation in other tissues like the liver and kidney. This selective targeting may be related to the integration of CD47 and α4/β1 acquired from membrane of macrophage. Histological examination of the aorta showed significant accumulation of Lipo-MM/DiD in AAA tissues, while Lipo/DiD accumulation was minimal (Figure 3G). These results confirmed the excellent ability of the Lipo-MM nanocarrier to activate VEC targeting and immune evasion in AAA.

Therapeutic Efficacy of SEI-Loaded Lipo-MM Nanoparticles Against AAA

To evaluate the therapeutic potential of SEI-loaded Lipo-MM nanoparticles in treating AAA, we conducted longitudinal studies in ApoE$^{-/-}$ male mice (8-week-old, n=10/group) with AngII-induced AAA pathology. A 28-day continuous AngII infusion (1000ng/kg/min) was administered using subcutaneously implanted mini-osmotic pumps, alongside weekly intravenous doses (35 mg/kg) of therapeutic agents (PBS, SEI, Lipo/SEI, or Lipo-MM/SEI).[22] Despite all groups developing AAA over a 4-week period (Figure 4A), quantitative morphometric analysis showed that administration of Lipo-MM/SEI significantly decreased 31.4% of maximum aortic diameter compared to controls ($p<0.01$, Figure 4B).

Notably, survival rates (2/10 vs 1/10) and AAA incidence (8/10 vs 7/10) showed no statistical significance between PBS, free SEI, and Lipo/SEI groups (Figure 4C), underscoring the necessity of targeted delivery. Administration of Lipo-MM/SEI significantly decreased AAA incidence to 40% compared with PBS and Lipo/SEI groups (Figure 4C). Histopathological evaluation demonstrated Lipo-MM/SEI's superior efficacy: H&E/EVG staining showed 58.7% attenuation of elastin degradation (Figure 4D and E), while immunofluorescence revealed preserved α-SMA expression (82.3% vs PBS group, Figure 4F). Concurrent TUNEL assays quantified 67.9% reduction in aortic apoptosis (Figure 4F and G), confirming sustained SEI release from Lipo-MM/SEI enhances anti-apoptotic effects through activated VEC targeting.

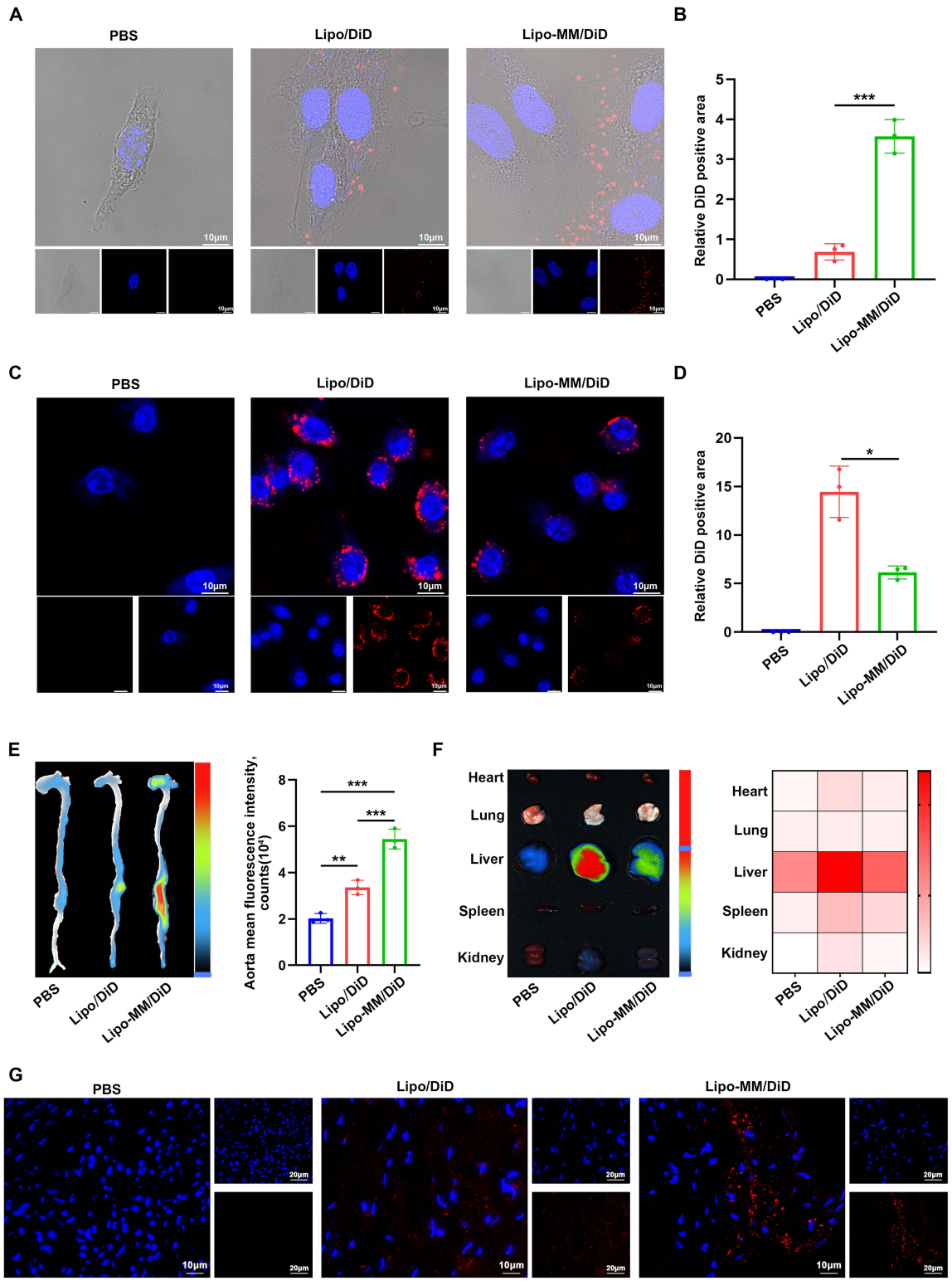

Figure 3 Anti-inflammatory efficacy of Lipo-MM NPs. (**A**) Cell uptake of Lipo/DiD NPs and Lipo-MM/DiD NPs after incubation with activated ECs (stimulated with TNF-α) for 4 h. The nuclei of activated ECs were stained with DAPI; scale bar =10μm. (**B**) Quantification of the DiD-positive area in activated ECs (mean±SD, n=3). One-way ANOVA with Bonferroni's multiple comparisons test. (**C**) Cell uptake of Lipo/DiD NPs and Lipo-MM/DiD NPs after incubation with macrophages. The nuclei of activated macrophages were stained with DAPI; scale bar = 10 μm. (**D**) Quantification of the DiD-positive area in activated macrophages (mean±SD, n=3). One-way ANOVA with Bonferroni's multiple comparisons test. (**E**) Representative ex vivo fluorescence images of DiD fluorescence dye accumulated in the aorta at 24 h after intravenous injection of Lipo/DiD NPs or Lipo-MM/DiD NPs (mean±SD, n=3). Quantitative data of DiD fluorescence dye in the aorta (mean±SD, n=3). One-way ANOVA with Bonferroni's multiple comparisons test. (**F**) Representative ex vivo fluorescence images of DiD fluorescence dye accumulation in different organs at 24 h after intravenous injection of Lipo/DiD NPs or Lipo-MM/DiD NPs (mean±SD, n=3, left). Heatmap of Dil fluorescence dye in different organs (mean±SD, n=3, right). (**G**) CLSM images of Lipo/DiD NPs and Lipo-MM/DiD NPs treated groups in the aortas of AAA mice (scale bar = 50μm and 25μm). Statistical significance is indicated as *P < 0.05; **P < 0.01; ***P < 0.001.

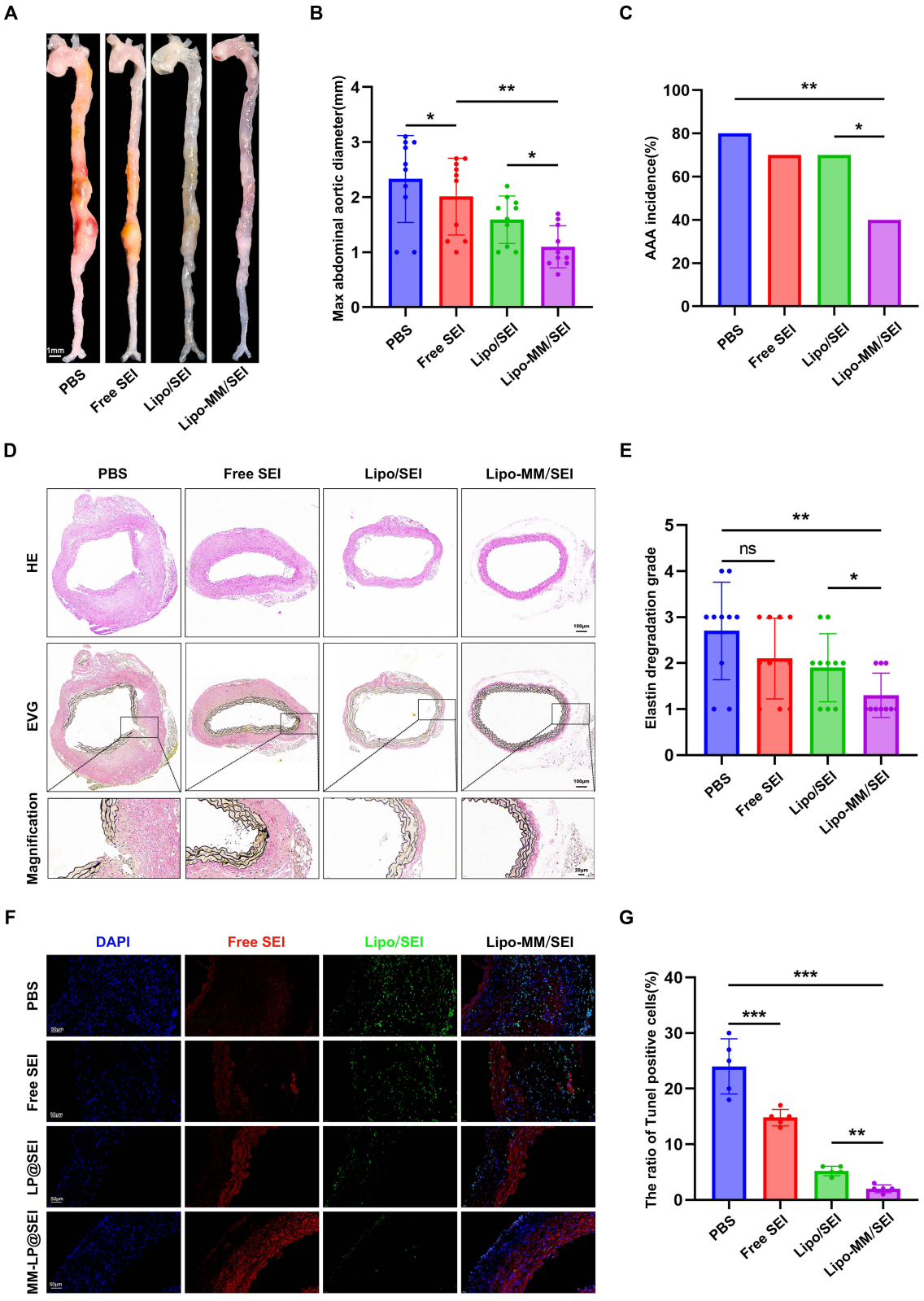

Figure 4 Anti-AAA Efficacy of the SEI-Loaded Lipo-MM. (**A**) Representative images showing the macroscopic features of aortas of AngII-induced AAA mice with different treatments. (**B**) Maximal diameter of abdominal aorta of AngII-induced AAA mice with different treatments. One-way ANOVA with Bonferroni's multiple comparisons test. (**C**) Aortic dissection incidence of AngII-induced AAA mice with different treatments. One-way ANOVA with Bonferroni's multiple comparisons test. (**D**) Representative images showing HE (top) and EVG (10×, middle and 40×, bottom) staining in the abdominal aorta from the indicated groups. (**E**) Elastin degradation score of abdominal aorta of AngII-induced AAA mice with different treatments. One-way ANOVA with Bonferroni's multiple comparisons test. (**F**) Representative images showing Immunofluorescence staining of α-SMA and TUNEL staining of abdominal aorta of AngII-induced AAA mice with different treatments. (**G**) The ratio of TUNEL positive cell of abdominal aorta of AngII-induced AAA mice with different treatments. One-way ANOVA with Bonferroni's multiple comparisons test. Statistical significance is indicated as *P < 0.05; **P < 0.01; ***P < 0.001.

https://doi.org/10.2147/IJN.S565290

Anti-Inflammatory Efficacy of Lipo-MM

Intense inflammatory responses are frequently linked to cardiovascular diseases, such as myocardial infarction and ischemia-reperfusion injury and atherosclerosis18-20. Excessive inflammation significantly contributes to the rapid progression of AAA. The Lipo-MM nanodrug delivery system effectively adsorbs inflammatory factors due to its macrophage membrane-derived receptors, including LTR4, CD126, and CD119. Once we verified the presence of essential receptors that attach to inflammatory cytokines, we measured how effectively Lipo-MM nanoparticles could neutralize TNF-α, IL-1β, IL-6, and interferon-γ (IFN-γ) (Figure 5A). Cytokines were incubated with varying concentrations of Lipo-MM nanoparticles, and

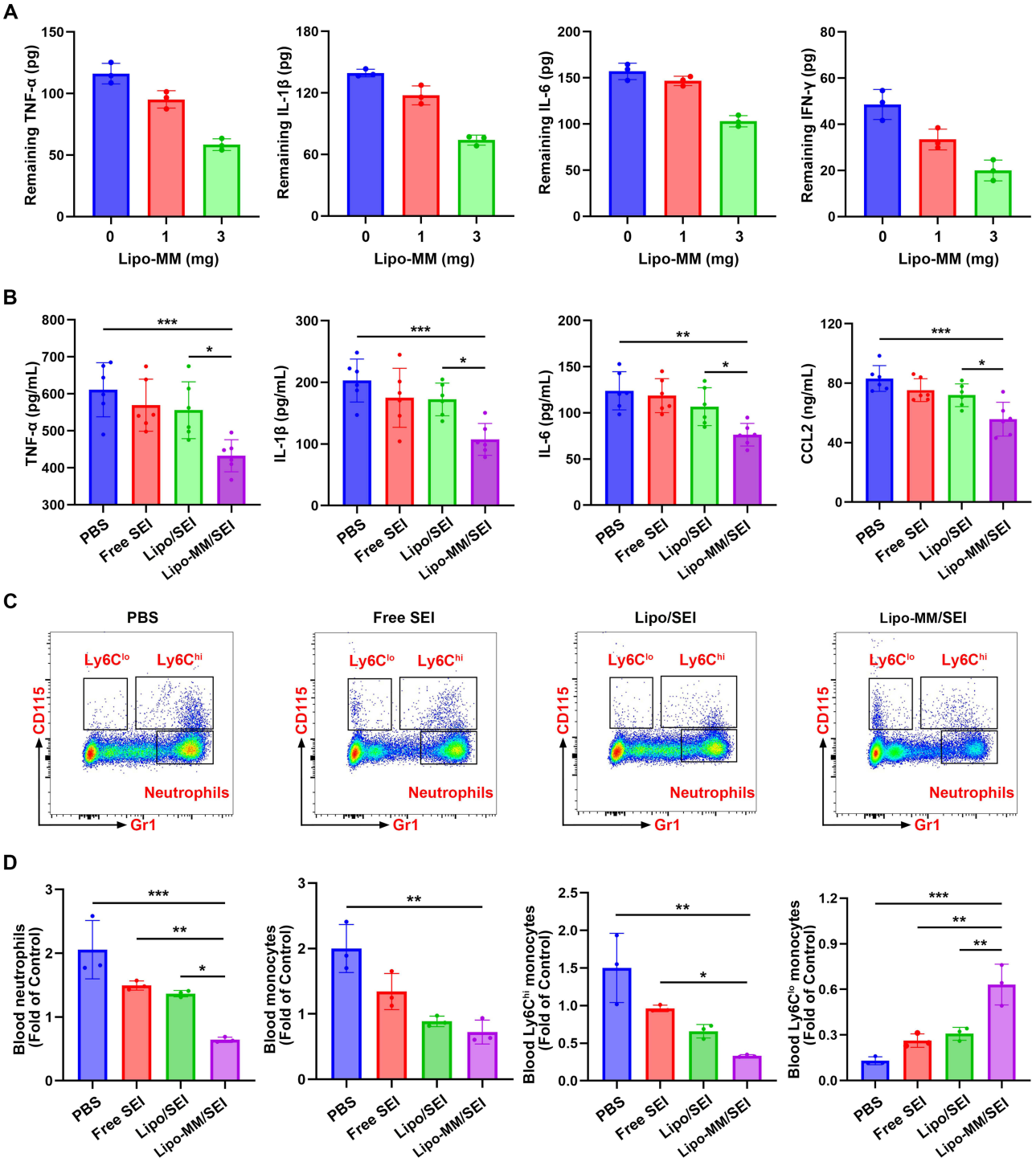

Figure 5 Continued.

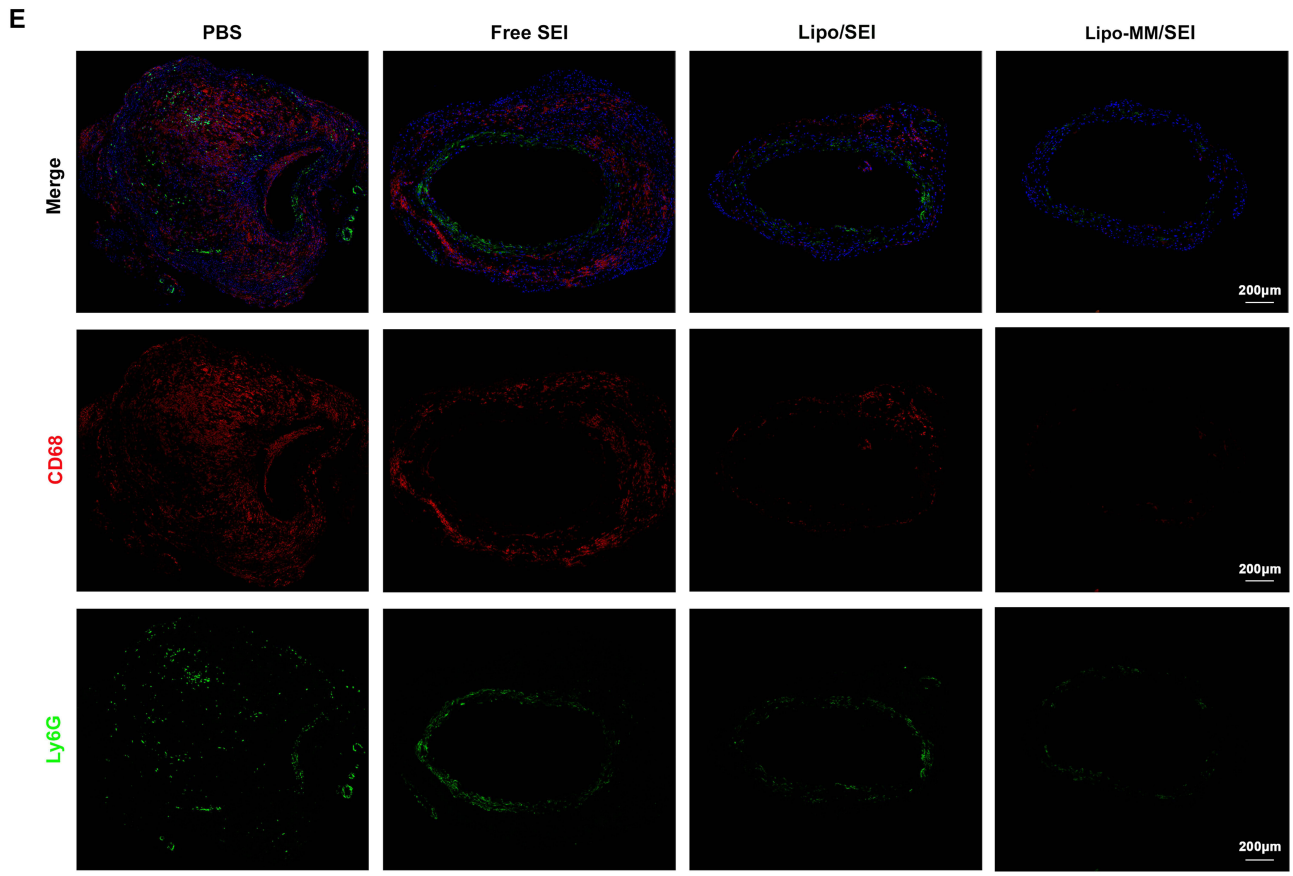

Figure 5 Anti-Inflammatory Efficacy of Lipo-MM/SEI. (**A**) Neutralization efficiencies of TNF-α, IL-1β, IL-6 and IFN-γ after incubation with Lipo-MM NPs (mean ± SD, n=3). One-way ANOVA with Bonferroni's multiple comparisons test. (**B**) ELISA analysis of the levels of the inflammatory factors TNF-α, IL-1β, IL-6 and CCL2 in murine serum from the different groups (n=6 per group). One-way ANOVA with Bonferroni's multiple comparisons test. (**C**) Representative flow cytometry analysis of circulating blood $Ly6C^{low}$, $Ly6C^{high}$ monocytes and Gr1+ neutrophils in different treatment groups. (**D**) Flow cytometry data analysis was performed as shown (n=3 per group). One-way ANOVA with Bonferroni's multiple comparisons test. (**E**) Representative images of frozen abdominal aorta sections in different treatment groups stained with Ly6G (green) and CD68 (red) while nuclei were stained with DAPI (blue). Scale bar =200μm. Statistical significance is indicated as *P < 0.05; **P < 0.01; ***P < 0.001.

ultracentrifugation was performed to eliminate the nanoparticles. Cytokine levels in the supernatant were subsequently quantified using ELISA. As the results demonstrated, as the dose of Lipo-MM increased (from 1 to 3 mg), the remaining levels of TNF-α decreased in an Lipo-MM dose-dependent manner. The findings indicated that Lipo-MM nanoparticles effectively neutralized the levels of these inflammatory cytokines (Figure 5A).

The neutralization capacity of Lipo-MM nanoparticles was assessed in AngII-induced AAA mice. Serum levels of inflammatory factors including IL-1β, IL-6, TNF-α, and CCL2 were significantly reduced in the Lipo-MM/SEI group (Figure 5B). The findings highlighted the essential function of Lipo-MM nanoparticles in mitigating AAA inflammation.

Peripheral blood was collected from each treatment group of mice to assess the impact of Lipo-MM/SEI on inflammatory cell recruitment. A comprehensive multicolor flow cytometry panel, including markers like CD11b, CD115, and GR1 for myeloid cells, was utilized. Blood flow cytometry analysis indicated a reduction in Ly6Chi monocytes and neutrophils in the Lipo-MM/SEI group compared to other groups (Figure 5C and D). The findings indicate that Lipo-MM/SEI both neutralized inflammatory factors and decreased the recruitment of pro-inflammatory cells in AAA mice (Figure 5E).

Mechanism of Lipo-MM/SEI

RNA-seq analysis was conducted on the model mouse aorta in both the free SEI and Lipo-MM/SEI groups to investigate the mechanisms by which Lipo-MM treats AAA (Figure 6A). Our findings indicated that, relative to the free SEI group, 43 genes were upregulated and 184 genes were significantly downregulated (Figure 6B and C). We conducted GO enrichment analysis

https://doi.org/10.2147/IJN.S565290

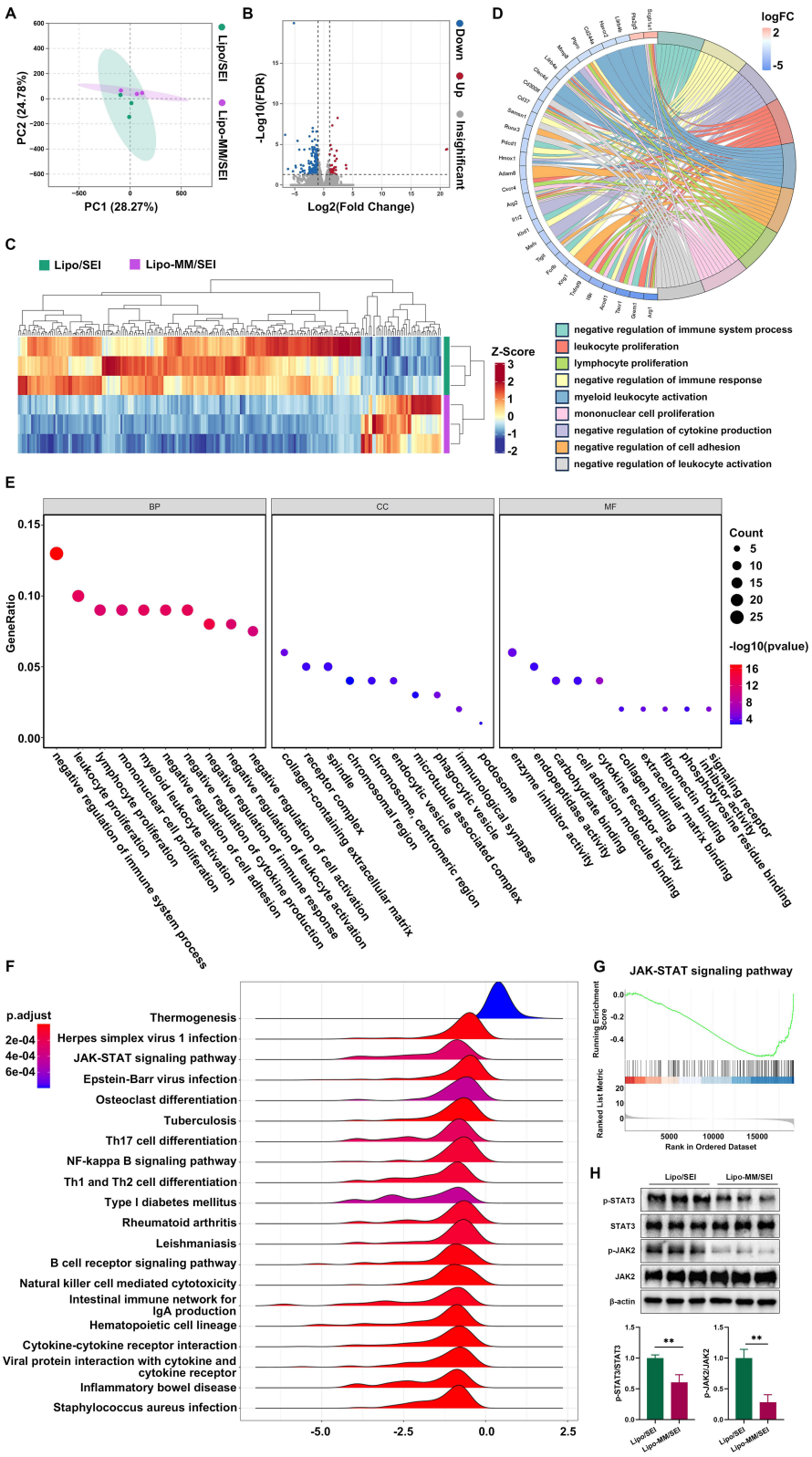

Figure 6 Potential mechanisms of Lipo-MM/SEI in treating AAA. (**A**) Principal component analysis (PCA) of RNA-seq data of aneurysmal aorta treated with free SEI or Lipo-MM/SEI. (**B**) Volcano plots of differently expressed genes (DEGs) between the free SEI and Lipo-MM/SEI groups in RNA-seq. (**C**) Hierarchical clustering analysis of DEGs between the free SEI and Lipo-MM/SEI groups. (**D**) The GO-enriched chord diagram shows the genes involved in nine significant enriched GO terms. (**E**) The bubble diagram shows the top 10 enriched molecular function, biological process and cellular compartment, respectively. (**F**) Ridge plots showing the top 20 KEGG pathways. (**G**) GSEA of JAK-STAT signaling pathway for free SEI vs Lipo-MM/SEI. (**H**) Representative Western blot images and quantitative analysis of STAT3, p-STAT3, JAK and p-JAK expression in aortic tissue (n = 3). Statistical significance is indicated as *P < 0.05; **P < 0.01; ***P < 0.001.

on the differentially expressed genes, revealing enrichment in inflammation-related pathways such as negative regulation of immune system processes, cytokine production, leukocyte activation, and cell adhesion (Figure 6D and E). The KEGG pathway analysis revealed enrichment in the JAK-STAT signaling pathway (Figure 6F). GSEA shows that JAK-STAT signaling pathway is down-regulated in the aorta tissue treated Lipo-MM/SEI vs free SEI (Figure 6G). These results reveal that Lipo-MM/SEI treats AAA via the JAK-STAT signaling pathway. Western blot analysis was performed on mouse aortic tissues revealing that the occurrence and progression of aortic dissection may be further improved by Lipo-MM/SEI through the down-regulated JAK-STAT signaling pathway (Figure 6H).

Biosafety Characteristics of Lipo-MM

Blood compatibility was assessed to evaluate the hemocompatibility of biological materials. Current study employed an in vitro direct contact method to assess the hemolysis of Lipos and Lipo-MMs. Clinical biochemistry analysis indicated that Lipo and Lipo-MM maintained normal kidney and liver functions, evidenced by standard levels of aspartate aminotransferase, alanine aminotransferase, serum creatinine, and blood urea nitrogen (Figure 7A).

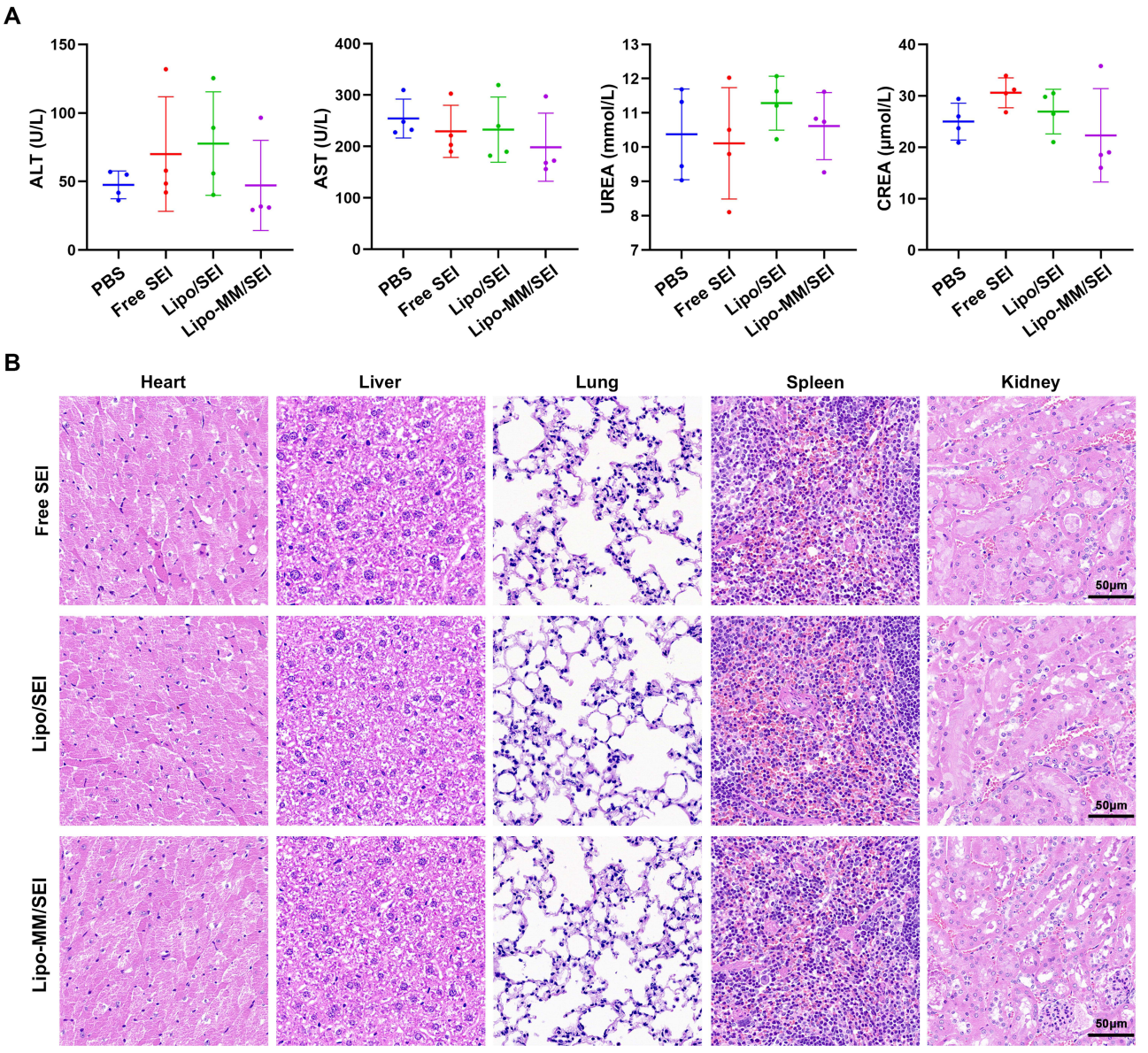

Figure 7 Biosafety Characteristics of Lipo-MM/SEI. (**A**) Serum level of ALT, AST, urea and creatinine of AngII-induced AAA mice with different treatments. One-way ANOVA with Bonferroni's multiple comparisons test. (**B**) Representative cross section from heart, liver,lung, spleen and kidney stained with H&E, scale bar = 50μm.

https://doi.org/10.2147/IJN.S565290

H&E staining was performed on tissue sections from various organs. Comparison of pathological sections of major organs from AAA mice revealed no significant differences between the control and various treatments (Figure 7B). The results revealed that Lipo-MMs as well as Lipos exhibit high biocompatibility in AAA mice following extended treatment.

Discussion

AAA is associated with a high mortality rate upon rupture. Currently, available treatments are restricted to either open surgery or endovascular stent grafting, both aimed at isolating the aneurysmal sac from systemic blood flow to prevent rupture. These interventions, however, are generally considered only for larger aneurysms (typically with a diameter exceeding 5.5cm), leaving a therapeutic gap for small AAAs, for which no effective approach exists to curb their progression. This shortage of treatment alternatives is partly attributable to an incomplete understanding of the early pathogenic mechanisms of AAA.

Early investigations into the pathogenesis of aortic aneurysms predominantly centered on the roles of medial smooth muscle cells and infiltrating inflammatory cells. In recent years, however, the focus has expanded to underscore the critical contributions of the endothelial layer. Endothelial cell dysfunction is now recognized as a pivotal early event in the development of aortic aneurysms. This dysfunction instigates a cascade of pathological processes, characterized by heightened oxidative stress and pronounced inflammation, which collectively drive the progressive degeneration of the arterial wall.[23] The influence of endothelial cells on aneurysm formation is largely mediated through their regulation of vascular remodeling. Evidence indicates that endothelial cells facilitate medial layer degradation and amplify the local inflammatory response via the secretion of various proteases and the recruitment of immune cells, including macrophages.[24] Furthermore, the activation of the NF-κB signaling pathway within endothelial cells constitutes a key mechanism. This activation leads to the upregulation of adhesion molecules, thereby promoting macrophage adhesion and transendothelial migration, which exacerbates the inflammatory milieu within the vessel wall.[25] The involvement of endothelial cells extends beyond these well-described roles in inflammation and remodeling. Hemodynamic forces, particularly shear stress, are transduced by endothelial cells and significantly impact arterial wall integrity. In response to altered flow dynamics, endothelial cells modulate inflammatory processes in the medial and adventitial layers through the paracrine release of cytokines and adhesion molecules, thereby influencing aneurysm initiation and expansion.[26] Adding another layer of complexity, recent studies highlight the functional heterogeneity of endothelial cells. Distinct transcriptional signatures identified in different endothelial subpopulations within aneurysmal tissues suggest specialized, and potentially spatially defined, roles in the disease pathogenesis. In conclusion, a compelling body of evidence now firmly establishes endothelial cells as central orchestrators in the pathogenesis of aortic aneurysms. Their dysfunction acts as a key driver of arterial wall degradation and inflammation, while also critically modulating vascular remodeling and intercellular signaling. Consequently, targeting endothelial cell-specific pathways emerges as a promising strategic avenue for devising novel therapeutic interventions aimed at halting the progression of aortic aneurysms.

Natural compounds derived from medicinal plants have long served as a rich resource for drug discovery, with notable successes such as aspirin, artemisinin, and paclitaxel. SEI, a primary active component of Ligusticum sinense ‘Chuanxiong’, has been found to exhibit anti-inflammatory, analgesic, antioxidant, and antithrombotic activities, as well as protective effects against ischemia-reperfusion injury. Prior studies found SEI inhibited inflammation and oxidative stress to restore endothelial function and vascular homeostasis, thus prevented TAAD formation in mice.[27] Compared with chemical compound, SEI shows the advantage of established safety and drug tolerability.[28] We found that Lipo-MM/SEI protects against AAA, likely by inhibiting the JAK-STAT pathway within the aortic tissue. This proposition is corroborated by existing evidence that SEI inhibits JAK1/3-STAT3/6 and JNK signaling.[29] The use of a nano-encapsulation system enhanced the targeted delivery of SEI to the abdominal aorta, which in turn augmented the suppression of the JAK-STAT pathway and the overall therapeutic effect.

Nanoscience enables the development of targeted drug delivery systems. To this end, multifunctional nanoparticles can be engineered with specific ligands or biomembranes to direct therapeutic agents to the lesion site, thereby minimizing systemic toxicity. Moreover, NP-based delivery enhances key pharmacological properties of drugs, including

their solubility, circulation half-life, bioavailability, and overall therapeutic efficacy. Through judicious design, these nano-biomaterials can achieve prolonged stability within the vasculature, effectively evading cellular uptake.

Previous studies have established various membrane-hybrid nanoparticles for biomedical applications. For instance, red blood cell-mimicking nanoparticles exhibit prolonged circulation, reduced immunogenicity, and specific targeting capacity, offering a promising drug delivery platform.[20] Polymeric nanoparticles coated with neutrophil membranes retain the antigenic and functional profiles of the source cells, enabling targeted accumulation in inflammatory joint regions.[30] Similarly, platelet membrane-coated nanoparticles-using membrane fragments rather than live platelets-show extended circulation and an inherent ability to bind injured endothelial cells via surface adhesion motifs, facilitating targeted delivery to thrombotic sites owing to the natural homing properties of platelets.[31]

In contrast to acute thrombotic events, AAA progression is characterized by chronic inflammation. This process drives aneurysm expansion through sustained extracellular matrix degradation and recruitment of pro-inflammatory cells, often marked by an elevated M1/M2 macrophage ratio. Within this context, MMs offer superior biocompatibility over synthetic coatings and can evade nonspecific macrophage uptake, thereby prolonging nanocarrier retention in inflamed tissues. Moreover, MMs are enriched with inflammation-related receptors-such as Toll-like receptors and interleukin-6 receptor families-which confer high affinity for inflammatory microenvironments and establish MMs as a superior inflammation-targeting nanocoating.

In the present study, we employed naturally derived macrophage membranes to overcome the limitations of poly (lactic-co-glycolic acid) nanoparticles. MM-coated nanoparticles exhibited reduced macrophage endocytosis, prolonged tissue retention, and enhanced accumulation at inflammatory sites. Additionally, similar to neutrophil membrane-coated systems, which are known to reduce immunogenicity and improve biocompatibility of synthetic nanoparticles after systemic administration, MM coating offers a biologically responsive strategy for enhancing the performance and safety of nanocarriers in chronic inflammatory settings such as AAA.

Future research should investigate the strategic integration of diverse biofilms, as such hybrid systems show considerable potential for constructing multifunctional targeted drug delivery platforms. These efforts could provide critical insights for advancing therapeutic strategies against AAA. Although Lipo-MM/SEI has demonstrated promising efficacy in our study, its clinical translation faces two principal challenges: the scalability of its fabrication process and the safety profile following long-term administration. While thin-film hydration represents a straightforward and widely adopted method for preparing deformable liposomes at the laboratory scale, it remains difficult to directly adapt this batch-based process for industrial-level manufacturing. A recognized limitation of our membrane-coating process (eg, co-extrusion) is its stochastic nature, which can result in heterogeneous orientations of key membrane proteins (eg, chemokine receptors) on the final nanoparticles. This heterogeneity could, in theory, impact the consistency of targeting efficacy across different Lipo-MM/SEI batches. Nevertheless, our in vitro and in vivo data confirm consistent and effective targeting, demonstrating that the functional integrity is preserved despite potential variations. To fundamentally overcome this limitation and enhance reproducibility, future work will pursue directed fusion strategies, such as introducing specific molecular anchors (eg, streptavidin-biotin) to control orientation. In addition, comprehensive large-animal studies are essential to systematically evaluate the long-term biosafety of Lipo-MM/SEI before clinical application.

Conclusion

This study developed a n new nanodrug carrier system Lipo-MMs, leveraging both advantages to achieve prolonged targeting of activated ECs in vivo. Studies conducted in vitro indicated that Lipo-MM nanoparticles effectively attached to activated endothelial cells and reduced macrophage phagocytosis. Additionally, the therapeutic efficacy of the hybrid system was explored in a mouse model of abdominal aortic aneurysm (AAA), where extended intravenous delivery of Lipo-MM/SEI nanoparticles led to a significant enhancement in AAA outcomes.

Summary

A novel hybrid biomimetic nanovesicle fusing macrophage membranes with artificial lipid bilayers was developed to deliver the endothelial-protective drug Senkyunolide I for the treatment of abdominal aortic aneurysm. The platform

combines the natural targeting/inflammation-neutralizing capacity of macrophage membranes with the stability of synthetic lipids, establishing a promising prototype for precise vascular therapeutics with minimized off-target effects.

Acknowledgment

We acknowledge Liwen Bianji (Edanz) (https://www.liwenbianji.cn) for their assistance in editing the English text of this manuscript draft.

Author Contributions

All authors made a significant contribution to the work reported, whether that is in the conception, study design, execution, acquisition of data, analysis and interpretation, or in all these areas; took part in drafting, revising or critically reviewing the article; gave final approval of the version to be published; have agreed on the journal to which the article has been submitted; and agree to be accountable for all aspects of the work.

Funding

This research received funding from the Natural Science Foundation of China (grant numbers 82160072, 82400566), the Youth Project of the Natural Science Foundation of Hubei Province (grant numbers 2023AFB127), and the Enshi Prefecture Science and Technology Bureau, selenium citation special (grant numbers D20230072).

Disclosure

The authors declare no financial interests or personal relationships exist that could have influenced the current paper.

References

1. Cho MJ, Lee MR, Park JG. Aortic aneurysms: current pathogenesis and therapeutic targets. *Exp Mol Med*. 2023;55:2519–2530. doi:10.1038/s12276-023-01130-w
2. Yang G, Khan A, Liang W, Xiong Z, Stegbauer J. Aortic aneurysm: pathophysiology and therapeutic options. *MedComm*. 2024;5(9):e703. doi:10.1002/mco2.703
3. Abadir PM, Foster DB, Crow M, et al. Identification and characterization of a functional mitochondrial angiotensin system. *Proc Natl Acad Sci USA*. 2011;108(36):14849–14854. doi:10.1073/pnas.1101507108
4. Cheng J, Zhang R, Li C, Tao H, Dou Y, Hu H. A Targeting Nanotherapy for Abdominal Aortic Aneurysms. *J Am College Cardiol*. 2018;72(21):2591–2605. doi:10.1016/j.jacc.2018.08.2188
5. Gao J, Cao H, Hu G, et al. The mechanism and therapy of aortic aneurysms. *Signal Transduct Target Ther*. 2023;8:55. doi:10.1038/s41392-023-01325-7
6. Yu J, Yang YN, Chen W, et al. Role of gut microbiota and derived metabolites in cardiovascular diseases. *iScience*. 2025;28:113247.
7. Golledge J, Thanigaimani S, Powell JT, Tsao PS. Pathogenesis and management of abdominal aortic aneurysm. *Eur Heart J*. 2023;44(29):2682–2697. doi:10.1093/eurheartj/ehad386
8. Li Y, Yu J, Wang Y. Mechanism of Coronary Microcirculation Obstruction after Acute Myocardial Infarction and Cardioprotective Strategies. *Rev cardiovasc med*. 2024;25(10):367. doi:10.31083/j.rcm2510367
9. Yu J, Li Y, Hu J, Wang Y. Interleukin-33 induces angiogenesis after myocardial infarction via AKT/eNOS signaling pathway. *Int Immunopharmacol*. 2024;143:113433. doi:10.1016/j.intimp.2024.113433
10. Lederman RJ, Greenbaum AB, Khan JM, Bruce CG, Babaliaros VC, Rogers T. Transcaval Access and Closure Best Practices. *JACC: Cardiovasc Interv*. 2023;16(4):371–395. doi:10.1016/j.jcin.2022.12.005
11. Li Y, Yu J, Chen W, et al. 12-HETE Is an Endogenous Modulator of BLT2 Triggering Vascular Degeneration, Dissection, and Rupture. *Adv Sci*. 2025;e15897. doi:10.1002/advs.202515897
12. Li Y, Ren P, Dawson A, et al. Single-Cell Transcriptome Analysis Reveals Dynamic Cell Populations and Differential Gene Expression Patterns in Control and Aneurysmal Human Aortic Tissue. *Circulation*. 2020;142(14):1374–1388. doi:10.1161/CIRCULATIONAHA.120.046528
13. Kouroedov A, Eto M, Joch H, Volpe M, Lüscher TF, Cosentino F. Selective Inhibition of Protein Kinase Cβ 2 Prevents Acute Effects of High Glucose on Vascular Cell Adhesion Molecule-1 Expression in Human Endothelial Cells. *Circulation*. 2004;110(1):91–96. doi:10.1161/01.CIR.0000133384.38551.A8
14. Li Y, Che J, Chang L, et al. CD47- and Integrin α4/β1-Comodified-Macrophage-Membrane-Coated Nanoparticles Enable Delivery of Colchicine to Atherosclerotic Plaque. *Adv Healthc Mater*. 2022;11:e2101788.
15. Baman JR, Eskandari MK. What Is an Abdominal Aortic Aneurysm? *JAMA*. 2022;328(22):2280. doi:10.1001/jama.2022.18638
16. Hellenthal FA, Buurman WA, Wodzig WK, Schurink GW. Biomarkers of abdominal aortic aneurysm progression. Part 2: inflammation. *Nat Rev Cardiol*. 2009;6(8):543–552. doi:10.1038/nrcardio.2009.102
17. Li Y, Wang J, Xie J. Biomimetic nanoparticles targeting atherosclerosis for diagnosis and therapy. *Smart Med*. 2023;2 e20230015.
18. Gu Y, Huang P, Cheng T, et al. A multiomics and network pharmacological study reveals the neuroprotective efficacy of Fu-Fang-Dan-Zhi tablets against glutamate-induced oxidative cell death. *Comput Biol Med*. 2022;148:105873. doi:10.1016/j.compbiomed.2022.105873

19. Yang Q, Zhao ZZ, Xie J, et al. Senkyunolide I attenuates hepatic ischemia/reperfusion injury in mice via anti-oxidative, anti-inflammatory and anti-apoptotic pathways. *Int Immunopharmacol*. 2021;97:107717. doi:10.1016/j.intimp.2021.107717
20. Li Y, Yu J, Cheng C, et al. Platelet and Erythrocyte Membranes Coassembled Biomimetic Nanoparticles for Heart Failure Treatment. *ACS nano*. 2024;18(39):26614–26630. doi:10.1021/acsnano.4c04814
21. Che J, Sun L, Shan J, et al. Artificial Lipids and Macrophage Membranes Coassembled Biomimetic Nanovesicles for Antibacterial Treatment. *Small*. 2022;18 e2201280.
22. Zhao K, Zhu H, He X, et al. Senkyunolide I ameliorates thoracic aortic aneurysm and dissection in mice via inhibiting the oxidative stress and apoptosis of endothelial cells. *Biochim Biophys Acta Mol Basis Dis*. 2023;1869(7):166819. doi:10.1016/j.bbadis.2023.166819
23. DeRoo E, Stranz A, Yang H, Hsieh M, Se C, Zhou T. Endothelial Dysfunction in the Pathogenesis of Abdominal Aortic Aneurysm. *Biomolecules*. 2022;13(1):12. doi:10.3390/biom13010012
24. Sun J, Deng H, Zhou Z, Xiong X, Gao L. Endothelium as a Potential Target for Treatment of Abdominal Aortic Aneurysm. *Oxid Med Cell Longev*. 2018;2018:6306542. doi:10.1155/2018/6306542
25. Saito T, Hasegawa Y, Yamada T, Gao J, Uno K, Ogihara T. Importance of endothelial NF-κB signalling in vascular remodelling and aortic aneurysm formation. *Cardiovascular Research*. 2013;97(1):106–114. doi:10.1093/cvr/cvs298
26. Spartalis E, Spartalis M, Athanasiou A, et al. Endothelium in Aortic Aneurysm Disease: new Insights. *Curr Med Chem*. 2020;27(7):1081–1088. doi:10.2174/0929867326666190923151959
27. Gao Y, Rong L, Cui J, et al. Artificial lipids and macrophage membranes coassembled biomimetic nanovesicles for thoracic aortic dissection treatment. *J Controlled Rel*. 2025;383:113844. doi:10.1016/j.jconrel.2025.113844
28. Wu SP, Wang N, Zhao L. Network Pharmacology Reveals the Mechanism of Activity of Tongqiao Huoxue Decoction Extract Against Middle Cerebral Artery Occlusion-Induced Cerebral Ischemia-Reperfusion Injury. *Front Pharmacol*. 2020;11:572624. doi:10.3389/fphar.2020.572624
29. Liu T, Wen T, Shen X, Xie C, Zhang R, Tian L. Senkyunolide I alleviates allergic rhinitis by inhibiting JAK1/3-STAT3/6 and JNK signalings. *Int Immunopharmacol*. 2025;165:115462. doi:10.1016/j.intimp.2025.115462
30. Zhang Q, Dehaini D, Zhang Y, et al. Neutrophil membrane-coated nanoparticles inhibit synovial inflammation and alleviate joint damage in inflammatory arthritis. *Nature Nanotechnol*. 2018;13(12):1182–1190. doi:10.1038/s41565-018-0254-4
31. Li Y, Xia Z, Xie Y, et al. Noninvasive platelet membrane-coated Fe 3 O 4 nanoparticles identify vulnerable atherosclerotic plaques. *Smart Medicine*. 2024;3(2):e20240006. doi:10.1002/SMMD.20240006